

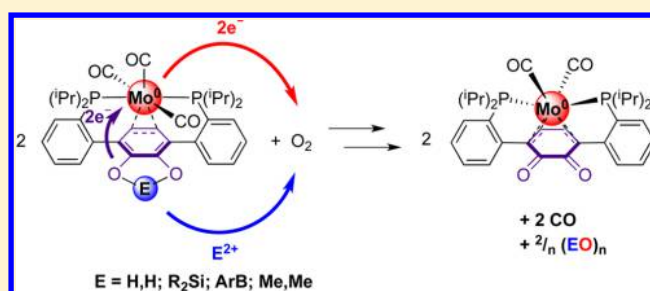
Combination of Redox-Active Ligand and Lewis Acid for Dioxygen Reduction with π -Bound Molybdenum–Quinonoid Complexes

Justin T. Henthorn, Sibio Lin, and Theodor Agapie*

Division of Chemistry and Chemical Engineering, California Institute of Technology, 1200 East California Boulevard, MC 127-72, Pasadena, California 91125, United States

Supporting Information

ABSTRACT: A series of π -bound Mo–quinonoid complexes supported by pendant phosphines have been synthesized. Structural characterization revealed strong metal–arene interactions between Mo and the π system of the quinonoid fragment. The Mo–catechol complex (2a) was found to react within minutes with 0.5 equiv of O₂ to yield a Mo–quinone complex (3), H₂O, and CO. Si- and B-protected Mo–catecholate complexes also react with O₂ to yield 3 along with (R₂SiO)_n and (ArBO)₃ byproducts, respectively. Formally, the Mo–catecholate fragment provides two electrons, while the elements bound to the catecholate moiety act as acceptors for the O₂ oxygens. Unreactive by itself, the Mo–dimethyl catecholate analogue reduces O₂ in the presence of added Lewis acid, B(C₆F₅)₃, to generate a Mo^I species and a bis(borane)-supported peroxide dianion, [[(F₅C₆)₃B]₂O₂²⁻], demonstrating single-electron-transfer chemistry from Mo to the O₂ moiety. The intramolecular combination of a molybdenum center, redox-active ligand, and Lewis acid reduces O₂ with pendant acids weaker than B(C₆F₅)₃. Overall, the π -bound catecholate moiety acts as a two-electron donor. A mechanism is proposed in which O₂ is reduced through an initial one-electron transfer, coupled with transfer of the Lewis acidic moiety bound to the quinonoid oxygen atoms to the reduced O₂ species.



1. INTRODUCTION

Biological reduction of dioxygen is performed by active sites that employ redox-noninnocent ligands and proton relays to control the transfer of electrons and protons to the substrate.¹ In synthetic transition-metal chemistry, redox-noninnocent ligands² and second-coordination-sphere acid/base moieties that facilitate proton transfer³ engender novel reactivity at the metal center. However, ligand systems that engage in both electron and proton transfers to substrates are less common.⁴ Metal–quinonoid complexes in which the metal is π -bound to the quinonoid fragment have the potential to access the two electrons and two protons of the hydroquinone/quinone couple in addition to any accessible metal-based redox couples. The study of π -bound metal–quinonoid complexes⁵ has focused on polymeric metal–organometallic coordination networks,⁵ with only rare examples of substrate-based reactivity.^{4b,6} Although not directly coordinated to a metal, hydroquinone has been employed as distal redox mediator.^{4b}

We have previously reported ligand designs that employ the π system of an arene to support metals in various coordination environments.⁷ A Ni–H complex underwent reversible migration of H between the metal and pendant arene, demonstrating the reversible transfer of (formally) protons and electrons between the Ni center and the ligand.⁸ Extending this chemistry to multiproton, multielectron processes at a single metal site with a pendant catechol moiety, we report herein the first synthesis of

a series of Mo–quinonoid complexes and their reactivity with dioxygen.

2. RESULTS AND DISCUSSION

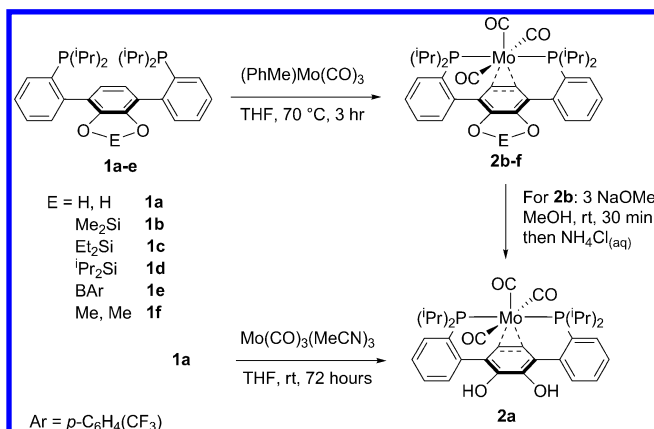
2.1. Synthesis and Characterization of π -Bound Mo–Quinonoid Complexes. Access to the desired Mo–catechol complex 2a was pursued through the use of the Si-protected catechol diphosphine 1b, designed to avoid the formation of oxygen-bound Mo–catecholate species. Heating diphosphine 1b with (PhMe)Mo(CO)₃ in tetrahydrofuran (THF) (Scheme 1) generates a new species 2b as determined by NMR spectroscopy. A singlet (50.6 ppm) is observed by ³¹P{¹H} NMR spectroscopy, while the protons assigned to the central arene ring in the ¹H NMR spectrum of 2b resonate upfield (5.7 ppm, CDCl₃) compared to the signal for the free phosphine 1b (6.8 ppm, CDCl₃) and have split into an apparent triplet (*J*_{HP} = 4 Hz). Additionally, two singlets account for the methyl groups bound to silicon, indicating desymmetrization of the two faces of the central ring. These data are consistent with a C_s-symmetric molecule in which there is a strong metal–arene interaction with the central ring of the terphenyl moiety. The solution IR spectrum of 2b reveals three bands in the region corresponding

Received: September 29, 2014

Revised: December 4, 2014

Published: January 10, 2015



Scheme 1. Synthesis of π -Bound Mo–Quinonoid Complexes

to CO stretches ($\nu_{\text{CO}} = 1959, 1843, \text{ and } 1835 \text{ cm}^{-1}$), consistent with a Mo(CO)_3 fragment.

The single-crystal X-ray diffraction (XRD) study of **2b** (Figure 1) confirmed the spectroscopic findings, which are also consistent with those for the previously reported analogue.⁹ In the solid state, the metal center exhibits a pseudo-octahedral geometry with the coordination sphere comprised of two trans phosphines, three meridional carbonyls, and an η^2 interaction with the π system of the catechol fragment. Localization of double-bond character in the central arene ring suggests significant π back-bonding between Mo and the ring (the $\text{C}_7\text{--C}_{12}$ and $\text{C}_{10}\text{--C}_{11}$ bonds at 1.37 \AA are considerably shorter than the $\text{C}_7\text{--C}_8$, $\text{C}_9\text{--C}_{10}$, and $\text{C}_{11}\text{--C}_{12}$ bonds at 1.43 \AA). The aryl C–O bond distances at 1.37 \AA are consistent with C–O single bonds.

The catechol complex **2a** can be accessed from **2b** by removal of the SiMe_2 group upon treatment with NaOMe in MeOH, followed by aqueous NH_4Cl workup. Alternatively, **2a** can be

accessed directly from diphosphine **1a** through reaction with $\text{Mo(CO)}_3(\text{MeCN})_3$ at room temperature. The resulting product exhibits spectroscopic features similar to those of **2b**. A new broad resonance at 5.6 ppm (^1H NMR) is assigned to the catechol OH protons. This assignment was confirmed by the loss of this resonance upon the addition of D_2O . An XRD study of **2a** (Figure 1) revealed structural parameters nearly identical to those of **2b**.

2.2. Reduction of O_2 by Mo–Catechol with Formation of Mo–Quinone. While transition-metal σ -bound catecholate complexes in general,^{1a,10} as well as Mo–catecholate complexes specifically,^{10b,11} have been reported to react with dioxygen to afford intra- and extra-diol cleavage products and oxidation to quinones, we are unaware of any reports on π -bound transition-metal–quinonoid complexes facilitating dioxygen reduction. To test the propensity of the metal–catechol moiety of **2a** to perform the transfer of multiple electrons and protons, its chemistry with O_2 was studied. Exposure of a solution of **2a** in dichloromethane (DCM) to an atmosphere of O_2 resulted in quantitative conversion to a new diamagnetic species **3** (eq 3) upon addition. The product displays a singlet at 72 ppm in the $^{31}\text{P}\{^1\text{H}\}$ NMR spectrum. In the ^1H NMR spectrum, the resulting species exhibits a new apparent triplet at 4.9 ppm , assigned to olefinic protons coupled to the phosphines. The solution IR spectrum of **3** reveals bands at 1875 and 1605 cm^{-1} , consistent with the stretching frequencies of a metal-bound carbonyl and a quinone carbonyl, respectively.¹² The solution $^{13}\text{C}\{^1\text{H}\}$ NMR spectrum reveals two resonances at ca. 240 ppm , consistent with two Mo-bound carbonyls. These spectroscopic features suggest conversion to a quinone– Mo(CO)_2 species, and this assignment was confirmed by an XRD study (Figure 1). The Mo center exhibits a pseudo-trigonal-prismatic geometry, with the vertices defined by two phosphine donors, two CO ligands, and two olefin moieties of the diene bound to the metal center in an η^4 fashion. The C–O bonds of the organic fragment have

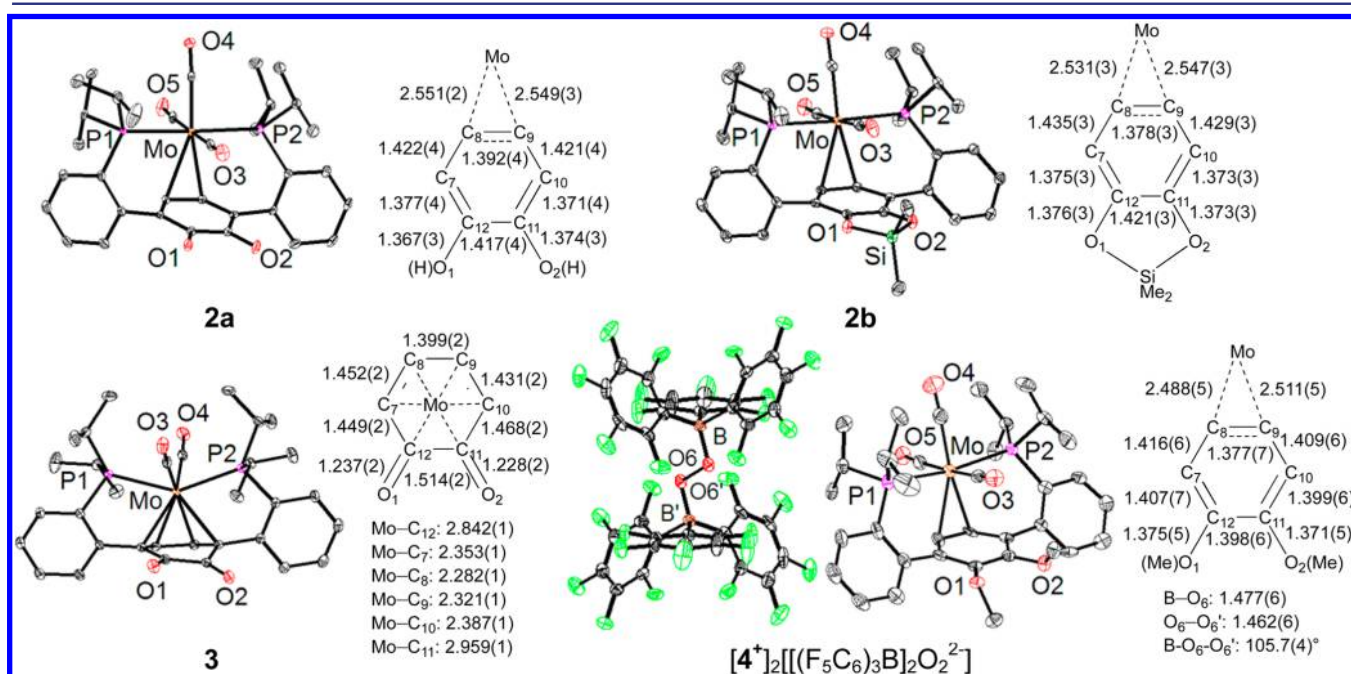
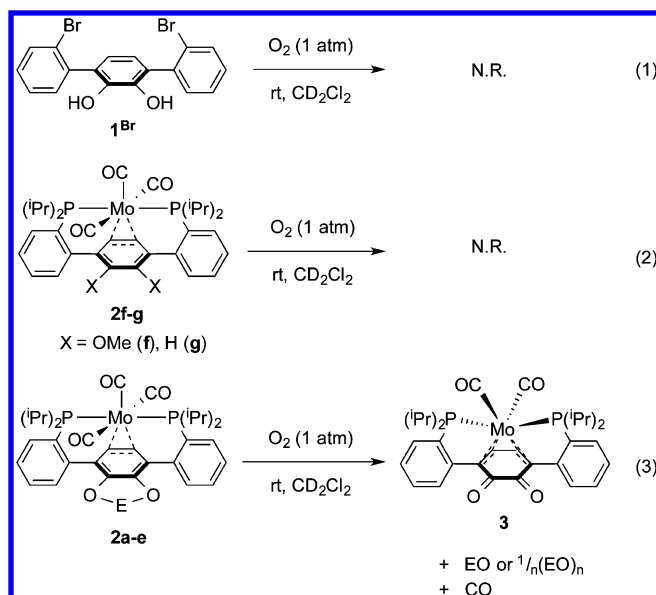


Figure 1. Solid-state structures of **2a**, **2b**, **3**, and $[\text{4}^+]_2[(\text{F}_5\text{C}_6)_3\text{B}]\text{O}_2^{2-}$. Solvent molecules, hydrogen atoms, and the second 4^+ cation have been omitted for clarity. Carbon and fluorine atoms are depicted in black and green, respectively. Selected bond distances (average values for the two molecules in the asymmetric unit for **2a**) are given in \AA .



contracted to 1.23 Å, consistent with carbon–oxygen double bonds. Formally, complex **2a** was oxidized by two electrons, coupled with the transfer of two protons, to generate **3**. In this net two-electron, two-proton transformation, the oxidation state of the metal center remains unchanged (Mo^0), with only the organic fragment undergoing the redox transformation.

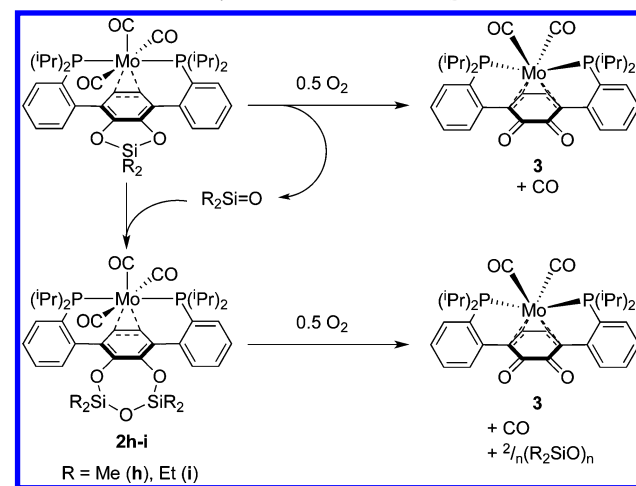
To deconvolute the effect of the catechol moiety versus the metal moiety in the reaction with O_2 , control experiments were performed with several species. 3,6-Bis(2-bromophenyl)catechol (**1Br**), a phosphine-free alternative to **1a**, exhibits no reaction under an atmosphere of O_2 in CD_2Cl_2 at room temperature, over 24 h as determined by ^1H NMR spectroscopy (eq 1). Under similar conditions, the dimethyl catecholate–Mo complex **2f** and the parent complex **2g** also showed no conversion with O_2 over 24 h (eq 2). These experiments indicate that the Mo–catechol combination is required for the observed reactivity.

Toepler pump experiments (see pp S25–S26 in the Supporting Information) were performed for the reaction of **2a** with 5 equiv of O_2 . A net increase in gas content of the sample was observed (0.48 ± 0.02 equiv per Mo) after quantitative conversion of **2a** to **3**. After removal of excess O_2 by reaction with a basic pyrogallol solution, the remaining gas was quantified (1.05 ± 0.05 equiv per Mo) and was found to be combustible with CuO at 350°C , consistent with CO . The identity of the released gas was further confirmed by its reaction with a Cu^{I} precursor to generate a previously reported $\text{Cu}^{\text{I}}(\text{CO})$ species.¹³ Overall, the Toepler pump experiments reveal that 0.5 equiv of dioxygen is consumed and 1 equiv of CO is released per mole of **2a**. This stoichiometry is consistent with four-electron reduction of O_2 to water involving 2 equiv of metal complex. This process could occur via partial reduction of O_2 to H_2O_2 by 1 equiv of **2a** followed by reduction of H_2O_2 with a second equivalent of **2a**. Indeed, **2a** is cleanly converted to **3** upon treatment with H_2O_2 , while **3** exhibits only minor conversion to unidentified species (<20%) with H_2O_2 (1 equiv) within 1 h. Thus, it is plausible that H_2O_2 could be the initial O_2 reduction product, which is then rapidly consumed by a second equivalent of **2a**.

To understand the O_2 reduction process in more detail, **2b** was investigated as a metal complex with an electron-rich central ring yet without easily transferable protons. Compound **2b** also reacts with O_2 to generate **3**, albeit slower than **2a** (over the course of several hours), with silyl-containing byproducts identified by

GC–MS as cyclo-oligomers of dimethylsiloxane. It has been reported that electrochemical reduction of O_2 in the presence of R_2SiX_2 ($\text{R} = \text{Me, Et, Ph}$; $\text{X} = \text{Cl, OMe}$) transiently generates silanones ($\text{R}_2\text{Si}=\text{O}$ species) that oligomerize to yield cyclopolysiloxanes.¹⁴ As silanones are highly reactive and rapidly oligomerize, the presence of silanones in solution is typically deduced via trapping experiments with linear siloxanes such as hexamethyldisiloxane.^{14,15} Silanones insert into the $\text{Si}-\text{O}$ bond of $\text{Me}_3\text{SiOSiMe}_3$ to yield longer-linear-chain siloxanes of the form $\text{Me}_3\text{Si}(\text{OSiMe}_2)_n\text{OSiMe}_3$ ($n = 1, 2$), which can be observed by GC–MS. Compound **2b** displays a $\text{Si}-\text{O}$ linkage for potential silanone insertion. Indeed, the intermediate species **2h** (Scheme 2) is observable by $^{31}\text{P}\{^1\text{H}\}$ and ^1H NMR spectroscopy

Scheme 2. Reactivity of **2b** and **2c** with O_2



during the reaction of **2b** with O_2 , with a relative integration of the $\text{Si}-\text{CH}_3$ singlets to the central arene triplet of 6:2 (rather than 3:2 as for **2b**). These data are consistent with insertion of generated $\text{Me}_2\text{Si}=\text{O}$ into the $\text{Si}-\text{O}$ bond of **2b** (Scheme 2), which was confirmed through independent synthesis. The observation of **2h** indicates that the Me_2Si moiety acts as an oxygen acceptor to generate $\text{Me}_2\text{Si}=\text{O}$, as protons do when starting from **2a** to generate $\text{H}_2\text{O}_2/\text{H}_2\text{O}$.

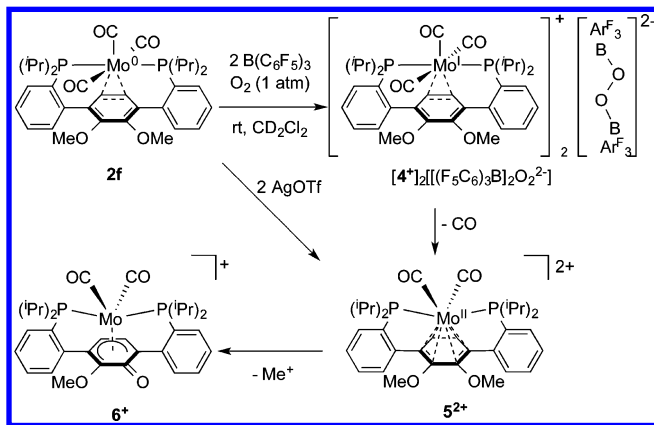
The effect of increasing the steric bulk at Si on the overall reaction with O_2 was investigated with the Et_2Si and $^i\text{Pr}_2\text{Si}$ analogues **2c** and **2d** (Scheme 1). Electrochemical measurements indicate that the nature of the alkyl group does not have a significant effect on the reduction potentials and hence the electronic properties of the complexes (see Figure 2 and Figure S73 in the Supporting Information). Exposure of **2c** to an atmosphere of O_2 leads to consumption of the starting material within hours, similar to **2b**, with the formation of a 1:1 mixture of **3** and the diethylsilanone insertion product **2i**; however, conversion of **2i** to **3** is slower, requiring 48 h for full conversion. The reaction of **2d** with O_2 is even slower than the conversion of **2i**, with a <20% yield of **3** generated over the course of 5 days at room temperature. The observed effect of steric bulk on reaction rate indicates that the silicon center is accessed during a rate-determining process; since the reduction potentials of **2b**, **2c**, and **2d** are very similar this process likely involves $\text{Si}-\text{O}$ bond formation from O_2 .

Reactivity with O_2 was found to extend to boron-substituted **2e** as well, though compared with **2b** the reaction is slower. After 36 h at room temperature, **2e** had been consumed and **3** formed in ca. 80% yield. New unidentified species were observed by

$^{31}\text{P}\{^1\text{H}\}$ NMR spectroscopy in addition to multiple broad resonances by ^{19}F NMR spectroscopy. A qualitatively similar set of spectra was obtained when **3** was combined with the boroxin $(\text{ArBO})_3$ in CD_2Cl_2 , likely as a result of the formation of Lewis acid–base adducts and 3-mediated oligomerization of an “ArBO” moiety similar to the polysiloxanes observed for **2b**.

2.3. Investigation of the Role of Lewis Acids in O_2 Reduction by Mo–Quinonoid Compounds. Considering that pendant H^+ , $[\text{R}_2\text{Si}]^{2+}$, and $[\text{RB}]^{2+}$ moieties can act as Lewis acids and that all engage in the O_2 activation process, more mechanistic insight was sought by addition of an external Lewis acid to target intermolecular reactivity. Compound **2f** does not exhibit O_2 reactivity on its own. Addition of 2 equiv of $\text{B}(\text{C}_6\text{F}_5)_3$ to **2f** under N_2 resulted in a broadening of the NMR spectroscopic features of **2f**, similar to what has been reported for a zirconocene complex.¹⁶ This may be caused by a combination of effects, including electron transfer and coordination of borane to ether or carbonyl moieties. Exposure of this mixture to O_2 affords a mixture that is silent by ^1H and $^{31}\text{P}\{^1\text{H}\}$ NMR spectroscopy, and a gradual color change from red-orange to brown to dark-purple ($\lambda_{\text{max}} = 575 \text{ nm}$) was observed over the course of 30 min at room temperature. Purple crystals of compound $[\text{4}^+]_2[[(\text{F}_5\text{C}_6)_3\text{B}]_2\text{O}_2^{2-}]$ were isolated from the reaction mixture (Scheme 3), and an XRD study

Scheme 3. Reactivity of **2f** with O_2 in the Presence of $\text{B}(\text{C}_6\text{F}_5)_3$



revealed a six-coordinate $\text{Mo}(\text{CO})_3$ unit bound by the terphenyl diphosphine with methoxy moieties intact, analogous to **2a** and **2b** (Figure 1). The unit cell contains a bis(borane)-supported peroxide dianion¹⁷ in a peroxide:Mo ratio of 1:2, indicating that the metal complex is a monocation (formally Mo^+), consistent with the lack of diamagnetic resonances by NMR spectroscopy. The formation of the $[[(\text{F}_5\text{C}_6)_3\text{B}]_2\text{O}_2^{2-}]$ dianion upon treatment of mixtures of ferrocenes and $\text{B}(\text{C}_6\text{F}_5)_3$ with O_2 was recently reported.¹⁷ The observation of $[\text{4}^+]_2[[(\text{F}_5\text{C}_6)_3\text{B}]_2\text{O}_2^{2-}]$ in the reaction of **2f** and $\text{B}(\text{C}_6\text{F}_5)_3$ with O_2 demonstrates the ability of the Mo center to reduce O_2 via outer-sphere one-electron transfer.

Over the course of several hours, the purple solution of 4^+ generated a new diamagnetic ion 5^{2+} , which was independently synthesized by oxidation of **2f** with 2 equiv of silver trifluoromethanesulfonate (AgOTf). Upon treatment of **2f** with AgOTf , the solution initially turned purple, consistent with the formation of the one-electron-oxidized product 4^+ , and then became pale-yellow-orange as 5^{2+} was produced via further oxidation and loss of CO. In the presence of the bis(borane)-supported peroxide dianion, 5^{2+} is partially converted to a new

diamagnetic species, 6^+ , resulting from ether demethylation. Independent synthesis by addition of MeOTf to **3** supports the structural assignment of 6^+ . After complete conversion of intermediate 4^+ to a mixture of 5^{2+} and 6^+ , vacuum transfer of the volatiles to a J. Young NMR tube revealed the formation of Me_2O and MeOH . To determine the origin of the O atom in Me_2O , the oxidation reaction was performed with $^{18}\text{O}_2$ instead of natural-abundance O_2 . Me_2O generated in the reaction was detected by GC–MS, and when the experiment was performed with $^{18}\text{O}_2$, the major isotopologue observed was Me_2^{18}O . While not quantitative, the observation of Me_2O formation suggests that the peroxide moiety reacts with 5^{2+} via abstraction of Me^+ to yield 6^+ .¹⁸ Conversion of 5^{2+} to 6^+ demonstrates the ability of a reduced oxygen species to cleave the O–element bond of the resulting oxidized Mo complex, although cleavage of the aryl–O bond has not been ruled out.^{18a}

The crystal structure of 4^+ allows for an evaluation of the effect of the metal oxidation state on the interaction with the arene. While partial localization of double-bond character in the catechol moiety was observed for **2a** and **2b**, with C–C distances varying between 1.37 and 1.43 Å, the dimethyl catecholate moiety of 4^+ displays C–C distances in a narrower range (1.40–1.42 Å). These structural parameters suggest that the Mo–arene interaction shifts from predominantly Mo-to-arene π back-bonding to arene-to-Mo σ donation upon oxidation of the metal center.¹⁹ The Mo–C distances are ca. 0.05 Å shorter in **2a** (ca. 2.55 Å) versus 4^+ (ca. 2.50 Å), indicating a strong interaction between the metal center and the ring. This interaction increases the electrophilicity of the arene and of the E group bonded to the catecholate oxygens. It is proposed that this activation of E for nucleophilic attack facilitates the reaction with the O_2 fragment.

Further insight into the redox chemistry of the reported Mo complexes was provided by cyclic voltammetry (CV) studies (Figure 2). Compound **2f** shows a symmetric and fairly reversible

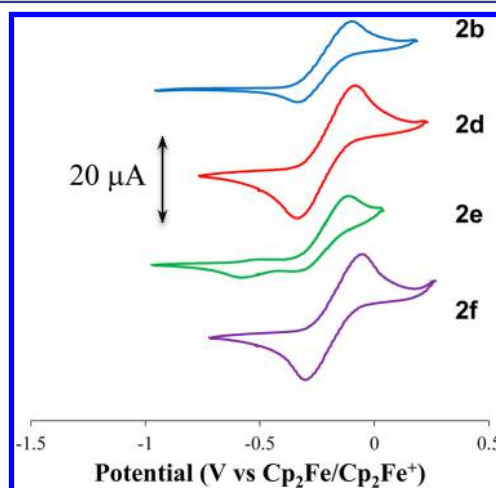


Figure 2. Cyclic voltammograms of compounds **2b** (blue), **2d** (red), **2e** (green), and **2f** (purple) in 0.1 M $[\text{n-Bu}_4\text{N}^+][\text{PF}_6^-]$ in THF recorded with a glassy carbon electrode at a scan rate of 100 mV/s. Potentials are referenced to $\text{Cp}_2\text{Fe}/\text{Cp}_2\text{Fe}^+$.

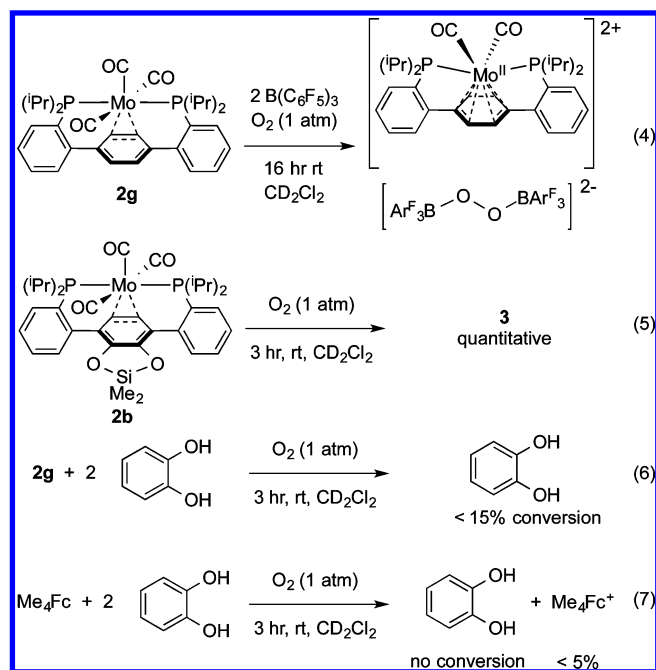
couple, consistent with the isolation of both neutral and oxidized species and relatively small structural reorganization. Compound **2b** exhibits a more asymmetric couple with lower cathodic current compared with anodic current. Increasing the steric bulk at Si in **2d** shows a return to a symmetric couple, while the more sterically accessible **2e** shows a fully irreversible couple at scan

rates between 50 and 2000 mV/s. This electrochemical behavior is reminiscent of the behavior of $(\eta^6\text{-arene})\text{Cr}(\text{CO})_3$ compounds, wherein the reversibility of the one-electron redox event is highly dependent on the presence of a nucleophile (an additive such as MeCN, MeOH, H₂O, or THF or the counteranion ClO_4^- or PF_6^-)^{20,21} because of chemical decomposition of the generated radical cation by external nucleophiles. Consequently, reversibility can be achieved in noncoordinating solvents such as CH_2Cl_2 by either lowering the temperature or employing less-nucleophilic electrolyte anions such as $[\text{B}(\text{C}_6\text{F}_5)_4]^-$.²¹

For compounds **2b–e**, we speculate that upon one-electron oxidation, the Si or B bound to the catecholates oxygens develops more electrophilic character and becomes susceptible to attack by an external nucleophile, either from the supporting electrolyte (tetrabutylammonium hexafluorophosphate) or even the solvent itself (THF), resulting in the observed electrochemical irreversibility. Indeed, chemical oxidation of **2b** with either 1 or 2 equiv of $\text{Ag}(\text{OTf})$ or $[\text{Cp}_2\text{Fe}^+][\text{PF}_6^-]$ in THF resulted in a mixture of species (as determined by ^1H and $^{31}\text{P}\{^1\text{H}\}$ NMR spectroscopy) that is capable of polymerizing THF over the course of several hours, suggesting the generation of a very electrophilic species. Conversely, the oxidation of **2d** with 2 equiv of $\text{Ag}(\text{OTf})$ in THF yields a single major diamagnetic species as determined by ^1H and $^{31}\text{P}\{^1\text{H}\}$ NMR spectroscopy, and the resulting solution was not observed to polymerize THF. As the alkyl substituents bound to Si are oriented away from both the metal center and the catechol carbocyclic ring (Figure 1), the recovery of electrochemical reversibility in going from **2b** to **2d** and the lack of solvent polymerization upon chemical oxidation of **2d** suggest that Si is the site of nucleophilic attack. The bulkier isopropyl groups of **2d** better impede the approach of nucleophiles to the Si center compared with the methyl groups of **2b**. These results are consistent with the development of increased electrophilic character on the Lewis-acidic E upon oxidation, indicative of ligand–metal cooperation by activation of the catechol moiety upon Mo-based electron transfer. The reactivity of these species with O_2 follows the trends observed electrochemically, with the bulky species displaying more-reversible CV and reacting slower.

To further probe the role of metal–ligand (Mo–quinonoid) cooperativity for dioxygen reactivity, the reaction of **2g** with O_2 in the presence of external catechol was investigated. Compound **2g** was selected for this experiment to limit potential complications due to the loss of Me^+ , as were observed during the reaction of **2f** and $\text{B}(\text{C}_6\text{F}_5)_3$ with O_2 . Compound **2g** is competent for O_2 reduction in the presence of $\text{B}(\text{C}_6\text{F}_5)_3$, generating the same bis(borane)-supported peroxide, $[(\text{F}_5\text{C}_6)_3\text{B}]_2\text{O}_2^{2-}$, as **2f** according to ^{19}F NMR spectroscopy (eq 4).

Accordingly, exposure of an orange mixture of **2g** and catechol to an atmosphere of O_2 results in a slight darkening of the solution over the course of 3 h (the time required for quantitative conversion of **2b** to **3**; eq 5). $^{31}\text{P}\{^1\text{H}\}$ NMR spectroscopy shows a complete loss of signal, while ^1H NMR spectroscopy reveals a broadening of the signals corresponding to **2g**; however, the majority of the catechol remains unaffected over the course of the reaction (eq 6) with less than 15% conversion. After 36 h at room temperature, a new signal is observed by $^{31}\text{P}\{^1\text{H}\}$ NMR spectroscopy at 60 ppm, consistent with oxidation of the phosphine to free phosphine oxide, indicative of decomposition of the metal complex. These results suggest that the presence of external catechol is sufficient to facilitate O_2 reactivity at Mo. However, this is a slow process, and the low conversion of catechol and decomposition of the metal complex indicate that



the resulting reduced oxygen species preferentially reacts with the Mo complex over the external catechol. Additionally, the reaction of catechol with O_2 in the presence of 1,1',3,3'-tetramethylferrocene (Me_4Fc) as a surrogate outer-sphere reductant of similar potential as the reported Mo complexes was investigated (eq 7). Over the course of 3 h at room temperature, slight oxidation of Me_4Fc (<5%) was observed by UV–vis spectroscopy; however, no conversion of catechol was detected by ^1H NMR spectroscopy. The low conversion of catechol oxidation chemistry observed in these intermolecular reactions emphasizes the cooperative nature of the reactivity observed for the Mo–quinonoid complexes.

2.4. Proposed Mechanisms for O_2 Reduction by Mo–Quinonoid Complexes. The intermolecular reactivity of **2f** and O_2 in the presence of $\text{B}(\text{C}_6\text{F}_5)_3$ (Figure 3) offers insight applicable to the intramolecular systems. The proposed mechanism for O_2 activation by **2f** and $\text{B}(\text{C}_6\text{F}_5)_3$ initiates via outer-sphere electron transfer from Mo to O_2 facilitated by the strongly Lewis acidic borane. While the reduction potentials of the Mo^0/Mo^1 couple (-0.176 V in THF)²² and the $\cdot\text{O}_2^-/\text{O}_2$ couple (-1.18 V in dimethyl sulfoxide)²³ are mismatched, it has been demonstrated that electron transfer rates can be greatly increased by coupling to Lewis acid binding.²⁴ This pre-equilibrium step is driven forward by the rapid disproportionation of the proposed borane-supported superoxide into bis(borane)-supported peroxide and dioxygen, as has been previously reported.²⁵ Disproportionation of the formally 17-electron 4^+ yields the 18-electron complex **5**²⁺ and regenerates the starting material **2f**. While it is anticipated that the Mo^1 of **4**⁺ should be an even weaker reductant than **2f**, further oxidation of **4**⁺ via O_2 and $\text{B}(\text{C}_6\text{F}_5)_3$ to yield **5**²⁺ cannot be ruled out. η^6 coordination of phenol to a $\text{Cr}(\text{CO})_3$ unit resulted in a 4 pK_a unit increase in acidity,²⁶ and thus it is presumed that similar activation of the catecholate unit in **5**²⁺ results in increased susceptibility of the methyl groups toward nucleophilic attack. Both nucleophilic attack at the methyl carbon and at the aryl carbon have been proposed in $\text{Cp}^*\text{Ir}(\eta^6\text{-anisole})^+$ complexes.¹⁸ On the basis of our isotopic-labeling studies, **5**²⁺ is demethylated by the bis(borane)-supported peroxide via nucleophilic sub-

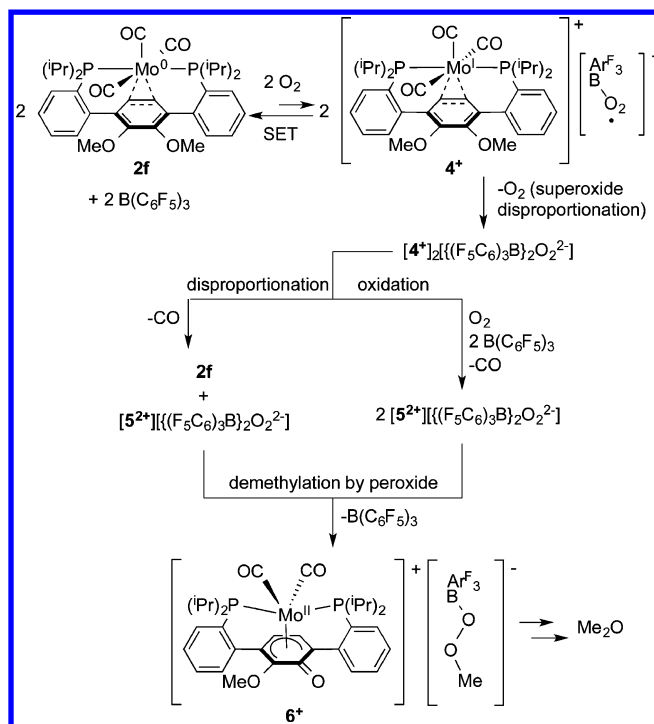


Figure 3. Proposed mechanism for the intermolecular reactivity of **2f** and $\text{B}(\text{C}_6\text{F}_5)_3$ with O_2 .

stitution at methyl to yield the methyl peroxide and 6^+ , with the former reacting further to yield the observed Me_2O or Me_2^{18}O .

For the catechol and Si- and B-protected catecholate π complexes, a related mechanism for O_2 activation is proposed (Figure 4A). Initial single-electron transfer is facilitated by binding of $\cdot\text{O}_2^-$ to the intramolecular Lewis acidic moiety E ($\text{E} = \text{H}, \text{R}_2\text{Si}, \text{ArB}$) as $\text{B}(\text{C}_6\text{F}_5)_3$ does with **2f** in intermolecular fashion.^{24a} The resulting intermediate **9** is an intramolecular analogue of putative $[4^+][(\text{F}_5\text{C}_6)_3\text{BO}_2^-]$. Oxidation of the Mo complex through electron transfer to O_2 results in increased electrophilicity at E, as supported by structural analysis of **4**⁺, electrochemical analysis, and chemical oxidation of **2b**. Loss of carbonyl coupled with attack by $\cdot\text{O}_2^-$ on the Lewis acid E results in scission of a catecholate–E bond, with subsequent steps leading to O–O bond cleavage (analogous to the formation of 6^+ and Me_2O). The intermediacy of Mo^{II} compound **10** accessed via further oxidation of **9** cannot be ruled out, with attack by a reduced oxygen species again resulting in formation of **11**. While it is unclear at which step the O–O bond is cleaved, one demonstrated possibility is that **2a** reduces H_2O_2 to yield H_2O and **3**. Analogous EO_2 species ($\text{E} = \text{R}_2\text{Si}, \text{ArB}$) are anticipated to be even more reactive than H_2O_2 , and it is therefore presumed that, if generated, they will be consumed via further reaction with starting material **2**. A recently computed mechanism for O_2 reduction with hydroanthraquinones invokes H atom abstraction,²⁷ and although the organoquinonoid **1**^{Br} does not react with O_2 , it cannot be ruled out that **2a** follows a similar mechanism (Figure 4B) wherein the Mo center does not directly participate in the reactivity but activates the catechol moiety.

3. CONCLUSIONS

In summary, π -bound Mo–catechol complexes were synthesized and their reactivity with dioxygen to yield a Mo–quinone product was investigated. Control experiments of Mo complexes in the absence of the catechol moiety or the catechol in the

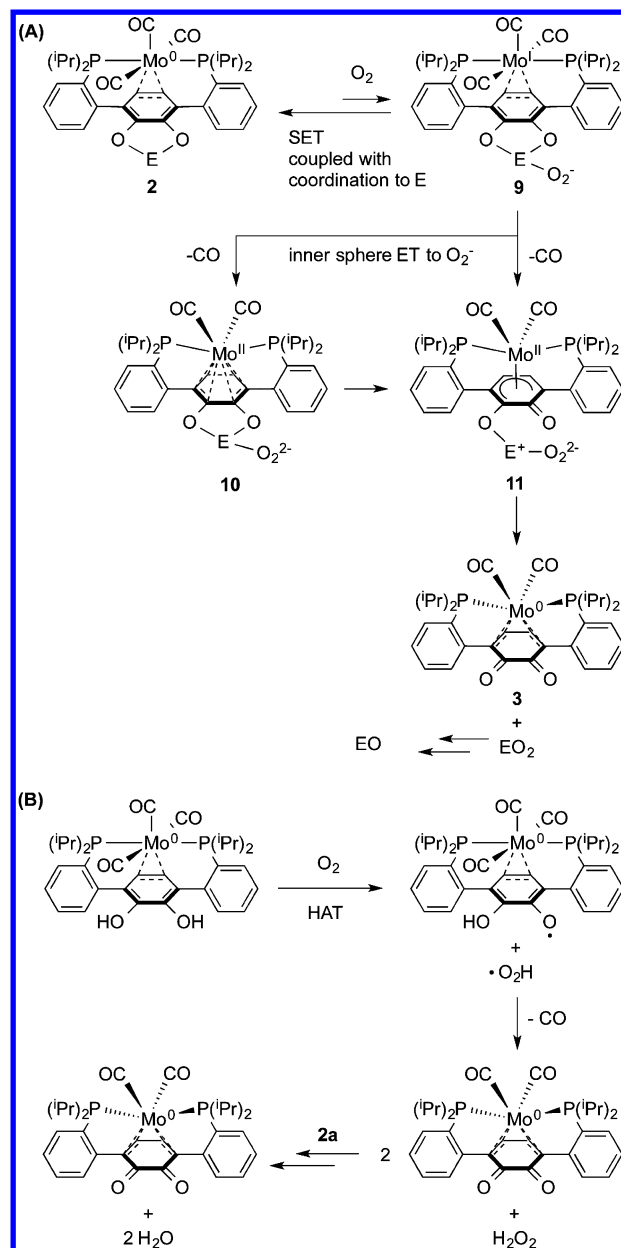


Figure 4. (A) Proposed mechanism for intramolecular reactivity of **2a–e,h,i** with O_2 . (B) Alternative mechanism for the intramolecular reaction of **2a** with O_2 .

absence of Mo showed no reaction with O_2 . Additionally, catechol added to solution but not covalently connected to Mo (or tetramethylferrocene as an alternate single-electron reductant) is oxidized only partially. Altering the substitution on the catechol oxygen centers from H to Si or B maintains the reactivity with O_2 , but at lower rates. The dimethyl Mo–quinonoid complex does not react with O_2 independently, but in the presence of $\text{B}(\text{C}_6\text{F}_5)_3$ affords a bis(borane)-supported peroxide. Mechanistically, the O_2 activation is proposed to occur via intramolecular Lewis acid-assisted electron transfer. The present studies demonstrate the ability of a π -bound metal–quinonoid complex to facilitate multielectron and proton transfer (as well as silicon, boron, and carbon transfer) from the quinonoid moiety to a small-molecule substrate and that coupling of the Mo and quinonoid fragments is integral to the observed reactivity. Current studies are focused on further exploiting this metal–

ligand cooperativity for O₂ reduction and extending it to other small molecules.

■ ASSOCIATED CONTENT

Supporting Information

Experimental procedures, characterization data, and crystallographic data (CIF). This material is available free of charge via the Internet at <http://pubs.acs.org>.

■ AUTHOR INFORMATION

Corresponding Author

*agapie@caltech.edu

Notes

The authors declare no competing financial interest.

■ ACKNOWLEDGMENTS

We thank Lawrence M. Henling and Dr. Michael Takase for crystallographic assistance, Prof. John E. Bercaw for providing access to a Toepler pump in his laboratory, and Christine Cheng for assistance in organic synthesis. We are grateful to Caltech and the NSF (CHE-1151918 to T.A.; GRFP to J.T.H.) for funding. T.A. is a Sloan, Cottrell, and Dreyfus Fellow. The APEX II X-ray diffractometer was purchased via an NSF CRIF:MU Award to Caltech (CHE-0639094).

■ REFERENCES

- (1) (a) Costas, M.; Mehn, M. P.; Jensen, M. P.; Que, L., Jr. *Chem. Rev.* **2004**, *104*, 939. (b) Whittaker, J. W. *Chem. Rev.* **2003**, *103*, 2347. (c) Sono, M.; Roach, M. P.; Coulter, E. D.; Dawson, J. H. *Chem. Rev.* **1996**, *96*, 2841.
- (2) (a) Luca, O. R.; Crabtree, R. H. *Chem. Soc. Rev.* **2013**, *42*, 1440. (b) Lyaskovskyy, V.; de Bruin, B. *ACS Catal.* **2012**, *2*, 270. (c) Praneeth, V. K. K.; Ringenberg, M. R.; Ward, T. R. *Angew. Chem., Int. Ed.* **2012**, *51*, 10228. (d) Eisenberg, R.; Gray, H. B. *Inorg. Chem.* **2011**, *50*, 9741. (e) Chirik, P. J.; Wieghardt, K. *Science* **2010**, *327*, 794. (f) Haneline, M. R.; Heyduk, A. F. *J. Am. Chem. Soc.* **2006**, *128*, 8410. (g) Pierpont, C. G. *Coord. Chem. Rev.* **2001**, *216–217*, 99. (h) Stanciu, C.; Jones, M. E.; Fanwick, P. E.; Abu-Omar, M. M. *J. Am. Chem. Soc.* **2007**, *129*, 12400.
- (3) (a) Umehara, K.; Kuwata, S.; Ikariya, T. *J. Am. Chem. Soc.* **2013**, *135*, 6754. (b) Carver, C. T.; Matson, B. D.; Mayer, J. M. *J. Am. Chem. Soc.* **2012**, *134*, 5444. (c) Hull, J. F.; Himeda, Y.; Wang, W.-H.; Hashiguchi, B.; Periana, R.; Szalda, D. J.; Muckerman, J. T.; Fujita, E. *Nat. Chem.* **2012**, *4*, 383. (d) Costentin, C.; Drouet, S.; Robert, M.; Savéant, J.-M. *Science* **2012**, *338*, 90. (e) Gunanathan, C.; Milstein, D. *Acc. Chem. Res.* **2011**, *44*, 588. (f) Rakowski DuBois, M.; DuBois, D. L. *Chem. Soc. Rev.* **2009**, *38*, 62. (g) Kohl, S. W.; Weiner, L.; Schwartsburd, L.; Konstantinovski, L.; Shimon, L. J. W.; Ben-David, Y.; Iron, M. A.; Milstein, D. *Science* **2009**, *324*, 74.
- (4) (a) Warren, J. J.; Tronic, T. A.; Mayer, J. M. *Chem. Rev.* **2010**, *110*, 6961. (b) Purse, B. W.; Tran, L.-H.; Piera, J.; Åkermark, B.; Bäckvall, J.-E. *Chem.—Eur. J.* **2008**, *14*, 7500. (c) Chang, C. J.; Chng, L. L.; Nocera, D. G. *J. Am. Chem. Soc.* **2003**, *125*, 1866. (d) Chaudhuri, P.; Hess, M.; Müller, J.; Hildenbrand, K.; Bill, E.; Weyhermüller, T.; Wieghardt, K. *J. Am. Chem. Soc.* **1999**, *121*, 9599. (e) Collman, J. P.; Devaraj, N. K.; Decréau, R. A.; Yang, Y.; Yan, Y.-L.; Ebina, W.; Eberspacher, T. A.; Chidsey, C. E. D. *Science* **2007**, *315*, 1565. (f) Lu, F.; Zarkesh, R. A.; Heyduk, A. F. *Eur. J. Inorg. Chem.* **2012**, 467.
- (5) (a) Kim, S. B.; Pike, R. D.; Sweigart, D. A. *Acc. Chem. Res.* **2013**, *46*, 2485. (b) Reingold, J. A.; Son, S. U.; Kim, S. B.; Dullaghan, C. A.; Oh, M.; Frake, P. C.; Carpenter, G. B.; Sweigart, D. A. *Dalton Trans.* **2006**, 2385.
- (6) Son, S. U.; Kim, S. B.; Reingold, J. A.; Carpenter, G. B.; Sweigart, D. A. *J. Am. Chem. Soc.* **2005**, *127*, 12238.
- (7) (a) Horak, K. T.; Velian, A.; Day, M. W.; Agapie, T. *Chem. Commun.* **2014**, *50*, 4427. (b) Herbert, D. E.; Lara, N. C.; Agapie, T. *Chem.—Eur. J.* **2013**, *19*, 16453. (c) Suseno, S.; Agapie, T. *Organometallics* **2013**, *32*, 3161. (d) Kelley, P.; Lin, S.; Edouard, G.; Day, M. W.; Agapie, T. *J. Am. Chem. Soc.* **2012**, *134*, 5480. (e) Velian, A.; Lin, S.; Miller, A. J. M.; Day, M. W.; Agapie, T. *J. Am. Chem. Soc.* **2010**, *132*, 6296.

- (8) Lin, S.; Day, M. W.; Agapie, T. *J. Am. Chem. Soc.* **2011**, *133*, 3828.
- (9) Buss, J. A.; Edouard, G. A.; Cheng, C.; Shi, J.; Agapie, T. *J. Am. Chem. Soc.* **2014**, *136*, 11272.
- (10) (a) Lippert, C. A.; Arnstein, S. A.; Sherrill, C. D.; Soper, J. D. *J. Am. Chem. Soc.* **2010**, *132*, 3879. (b) Morris, A. M.; Pierpont, C. G.; Finke, R. G. *J. Mol. Catal. A: Chem.* **2009**, *309*, 137. (c) Vaillancourt, F. H.; Bolin, J. T.; Eltis, L. D. *Crit. Rev. Biochem. Mol. Biol.* **2006**, *41*, 241. (d) Yin, C.-X.; Finke, R. G. *J. Am. Chem. Soc.* **2005**, *127*, 9003. (e) Barbaro, P.; Bianchini, C.; Mealli, C.; Meli, A. *J. Am. Chem. Soc.* **1991**, *113*, 3181.
- (11) (a) Randolph, A. H.; Seewald, N. J.; Rickert, K.; Brown, S. N. *Inorg. Chem.* **2013**, *52*, 12587. (b) Pierpoint, C. G.; Nordlander, E. In *Molybdenum: Its Biological and Coordination Chemistry and Industrial Applications*; Holder, A. A., Ed.; Nova Science Publishers: New York, 2012; p 161.
- (12) Campos, J. L.; De Giovanni, W. F.; Romero, J. R. *Synthesis* **1990**, 597.
- (13) Kretzer, R. M.; Ghiladi, R. A.; Lebeau, E. L.; Liang, H.-C.; Karlin, K. D. *Inorg. Chem.* **2003**, *42*, 3016.
- (14) (a) Keyrouz, R.; Jouikov, V. *New J. Chem.* **2003**, *27*, 902. (b) Fattakhova, D. S.; Jouikov, V. V.; Voronkov, M. G. *J. Organomet. Chem.* **2000**, *613*, 170.
- (15) (a) Hussman, G.; Wulff, W. D.; Barton, T. J. *J. Am. Chem. Soc.* **1983**, *105*, 1263. (b) Voronkov, M. G.; Basenko, S. V. *J. Organomet. Chem.* **1995**, *500*, 325.
- (16) Harlan, C. J.; Hascall, T.; Fujita, E.; Norton, J. R. *J. Am. Chem. Soc.* **1999**, *121*, 7274.
- (17) Henthorn, J. T.; Agapie, T. *Angew. Chem., Int. Ed.* **2014**, *53*, 12893.
- (18) (a) Miller, A. J. M.; Kaminsky, W.; Goldberg, K. I. *Organometallics* **2014**, *33*, 1245. (b) Amouri, H.; Vaissermann, J.; Rager, M. N.; Besace, Y. *Inorg. Chem.* **1999**, *38*, 1211.
- (19) Falceto, A.; Carmona, E.; Alvarez, S. *Organometallics* **2014**, *33*, 6660.
- (20) Geiger, W. E. *Coord. Chem. Rev.* **2013**, *257*, 1459.
- (21) (a) Stone, N. J.; Sweigart, D. A.; Bond, A. M. *Organometallics* **1986**, *5*, 2553. (b) Zoski, C. G.; Sweigart, D. A.; Stone, N. J.; Rieger, P. H.; Mocellin, E.; Mann, T. F.; Mann, D. R.; Gosser, D. K.; Doeff, M. M.; Bond, A. M. *J. Am. Chem. Soc.* **1988**, *110*, 2109.
- (22) All potentials are referenced to Cp₂Fe/Cp₂Fe⁺.
- (23) Maricle, D. L.; Hodgson, W. G. *Anal. Chem.* **1965**, *37*, 1562.
- (24) (a) Fukuzumi, S.; Ohkubo, K. *Coord. Chem. Rev.* **2010**, *254*, 372. (b) Fukuzumi, S.; Morimoto, Y.; Kotani, H.; Naumov, P.; Lee, Y.-M.; Nam, W. *Nat. Chem.* **2010**, *2*, 756. (c) Morimoto, Y.; Kotani, H.; Park, J.; Lee, Y.-M.; Nam, W.; Fukuzumi, S. *J. Am. Chem. Soc.* **2010**, *133*, 403. (d) Tarantino, K. T.; Liu, P.; Knowles, R. R. *J. Am. Chem. Soc.* **2013**, *135*, 10022.
- (25) Zheng, D.; Wang, Q.; Lee, H.-S.; Yang, X.-Q.; Qu, D. *Chem.—Eur. J.* **2013**, *19*, 8679.
- (26) Wu, A.; Biehl, E. R.; Reeves, P. C. *J. Chem. Soc., Perkin Trans. 2* **1972**, 449.
- (27) Nishimi, T.; Kamachi, T.; Kato, K.; Kato, T.; Yoshizawa, K. *Eur. J. Org. Chem.* **2011**, 4113.